Carbohydrate Polymers 92 (2013) 2033–2040

Contents lists available at SciVerse ScienceDirect

Carbohydrate Polymers

journal homepage: www.elsevier.com/locate/carbpol

Solid dispersion of quercetin in cellulose derivative matrices influences both solubility and stability

Bin Li[a], Stephanie Konecke[a], Kim Harich[b], Lindsay Wegiel[c], Lynne S. Taylor[c], Kevin J. Edgar[a,*]

[a] Department of Sustainable Biomaterials, Macromolecules and Interfaces Institute, and Institute for Critical Technology and Applied Sciences, Virginia Tech, Blacksburg, VA 24061, USA
[b] Department of Biochemistry, Virginia Tech, Blacksburg, VA 24061, USA
[c] Department of Industrial and Physical Pharmacy, College of Pharmacy, Purdue University, West Lafayette, IN 47907, USA

ARTICLE INFO

Article history:
Received 11 September 2012
Received in revised form
19 November 2012
Accepted 26 November 2012
Available online 3 December 2012

Keywords:
Quercetin
Amorphous solid dispersion
CMCAB
HPMCAS
Cellulose acetate adipate propionate
Bioavailability

ABSTRACT

Amorphous solid dispersions (ASD) of quercetin (Que) in cellulose derivative matrices, carboxymethylcellulose acetate butyrate (CMCAB), hydroxypropylmethylcellulose acetate succinate (HPMCAS), and cellulose acetate adipate propionate (CAAdP) were prepared with the goal of identifying an ASD that effectively increased Que aqueous solution concentration. Crystalline quercetin and Que/poly(vinylpyrrolidinone) (PVP) ASD were evaluated for comparison. Powder X-ray diffraction (XRPD) and differential scanning calorimetry (DSC) were used to examine the crystallinity of ASDs, physical mixtures (PM) and quercetin. ASDs were amorphous up to 50 wt% Que. Que stability against crystallization and solution concentrations from these ASDs were significantly higher than those observed for physical mixtures and crystalline Que. PVP stabilizes against both Que degradation and recrystallization; in contrast, these carboxylated cellulose derivatives inhibit recrystallization but release Que slowly. PVP ASDs afforded fast and complete drug release, while ASDs using these three cellulose derivatives provide slow, incomplete, pH-triggered drug release.

1. Introduction

Polyhydroxyaromatic flavonoids effectively protect body tissues against oxidative stress (Andersen & Markham, 2006; Rice-Evans & Packer, 2003). Quercetin (Que, Fig. 1) is an important dietary flavonoid, abundant in foods including onions and apples (Jan et al., 2010; Kelly, 2011). Recent work has shown that Que is much more than just a protective antioxidant; for example, it has been shown to enhance apoptosis of malignant cells, by itself (Chien et al., 2009) and in combination (Siegelin, Reuss, Habel, Rami, & von Deimling, 2009) with other molecules. Que has also been observed to exert anti-inflammatory, antibacterial, antiviral, and muscle-relaxation effects (Bischoff, 2008). Que can arrest cell cycles in both G1 and G2-M phases by inhibiting expression of p53 protein, affect xenobiotic metabolism, and also play a key role in signal transduction (Jan et al., 2010; Kuo, 2002; Lamson & Brignall, 2000). Recent reports indicate that Que may act both as antioxidant to improve normal cell survival and as pro-oxidant to induce apoptosis in cancerous cells (Gibellini et al., 2010; Lamson & Brignall, 2000; Murakami, Ashida, & Terao, 2008). The potential of Que as a cytotoxic anticancer agent has recently been augmented by the discovery, reviewed by Chen and co-workers, that Que may cause reversal of multidrug resistance (Chen, Zhou, & Ji, 2010). A great deal of effort has been devoted to the study of quercetin as a chemopreventive and chemotherapeutic agent (Jan et al., 2010).

Study and exploitation of these beneficial properties for therapeutic applications have been impeded by the fact that Que has poor aqueous solubility and low bioavailability. Que water solubility at room temperature and pH 3 was only ca. 400 ng/mL (Zheng, Haworth, Zuo, Chow, & Chow, 2005). It has been reported that dietary blood concentrations are in the 10^{-9} to 10^{-7} M range (Biasutto, Marotta, Garbisa, Zoratti, & Paradisi, 2010), while therapeutic antioxidant concentrations are in the range of 10^{-6} to 10^{-5} M (Vargas & Burd, 2010). Thus, realization of the therapeutic promise of quercetin requires enhancement of its solubility and oral bioavailability. The importance of quercetin as a potential therapeutic platform is illustrated by the efforts made to chemically modify Que to enhance solubility and bioavailability while retaining activity (Biasutto, Marotta, De Marchi, Zoratti, & Paradisi, 2006) Others have taken the drug delivery approach to enhance solubility and bioavailability of Que itself. Formation of Que/cyclodextrin inclusion complexes is a promising approach for increasing Que bioavailability (Zheng & Chow, 2009). Ribeiro et al. studied the effective solubilization of quercetin and rutin by micellar formulation with ethylene oxide triblock copolymers,

* Corresponding author at: 230 Cheatham Hall, Virginia Tech, Blacksburg, VA, 24061, USA. Tel.: +1 540 231 0674.
E-mail address: kjedgar@vt.edu (K.J. Edgar).

0144-8617/$ – see front matter © 2012 Elsevier Ltd. All rights reserved.
http://dx.doi.org/10.1016/j.carbpol.2012.11.073

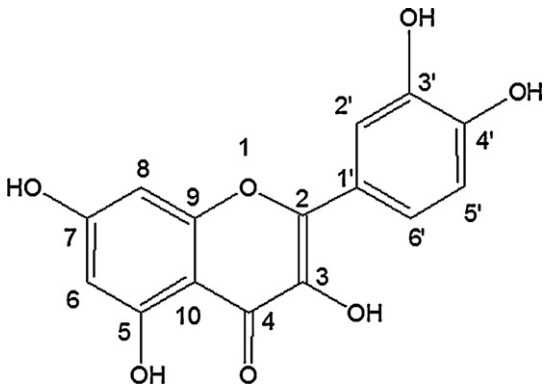

Fig. 1. Chemical structure of quercetin.

with solubilization exceeding that achieved with β-cyclodextrin (Ribeiro et al., 2009).

Amorphous solid dispersion (ASD) of quercetin is an interesting approach because of its effectiveness, simplicity, and benign nature. ASD is a very attractive way to improve drug solubility and bioavailability for oral delivery, which has been reviewed several times in the past decade (Leuner & Dressman, 2000; Qian, Huang, & Hussain, 2010; Singh, Sayyad, & Sawant, 2010; Timpe, 2010; Tiwari, 2009). Poor drug water solubility is often heavily influenced by high drug crystallinity, because the crystal lattice energy must be overcome for the drug to dissolve. Molecular dispersion of drug in a polymer provides amorphous drug, that when released may form a supersaturated solution. Selection or design of polymer structure is crucial to success (Ilevbare, Liu, Edgar, & Taylor, 2012), since the polymer must stabilize the metastable amorphous drug against crystallization in the solid dosage form, must dissolve in water to an extent adequate to stabilize the drug in supersaturated solution after release and prior to permeation through the enterocytes, and must release the drug at an adequate rate. Water-soluble polymers like PVP are most often employed in ASD studies, but there is increasing interest in polymers that swell in aqueous media like carboxylated polysaccharide derivatives. Polysaccharides generally have low toxicity, high glass transition temperatures (T_g) that promote formulation stability, and may be modified with ester and ether groups to enhance compatibility with drug and to introduce pH-responsiveness. Carboxyl-containing cellulose derivatives are particularly useful since the carboxyl provides specific interactions with drug functionality in addition to pH-triggered release; for example, hydroxypropylmethylcellulose acetate succinate (HPMCAS) (Friesen et al., 2008), cellulose acetate phthalate (CAPhth) (DiNunzio, Miller, Yang, McGinity, & Williams, 2008), and carboxymethylcellulose acetate butyrate (CMCAB) (Posey-Dowty et al., 2007; Shelton et al., 2009) have been used in ASDs to improve the water solubility and bioavailability of hydrophobic drugs. All three have promising properties, yet CAPhth has limited miscibility with drugs, CMCAB is prone to crosslinking, and HPMCAS is an excellent polymer for amorphous solid dispersion, and a component of multiple New Drug Applications before the Food and Drug Administration, yet is a very complex and potentially variable polysaccharide derivative.

There have been some reports of solubility enhancement of Que by solid dispersion. Polymer matrices used in these studies include poly(ethylene glycol) (PEG) (Li, Zhang, Deng, & Liang, 2004), PVP (Costa et al., 2011; Li, Yang, Bai, & Zhu, 2010; Zhu et al., 2007), and polysaccharide derivatives (Lauro, Maggi, Conte, De, & Aquino, 2005; Lauro, Torre, et al., 2002; Sansone et al., 2010). There have been only a few reports of Que solid dispersions using cellulose derivatives. Lauro et al. prepared quercetin and rutin gastroresistant microparticles by spray-drying using several polymers including cellulose acetate trimellitate (CAT) and CAPhth as matrix polymers (Lauro, Maggi, et al., 2005; Lauro, Torre, et al., 2002). Recently Sansone et al. also reported that the microparticles of quercetin and CAPhth prepared by spray drying may enhance Que stability and dissolution rate (Sansone et al., 2010). Que dispersions in CMCAB and HPMCAS matrices have not been reported.

Herein we report studies of the effect on Que stability and solubility enhancement of preparing Que solid dispersions, comparing three cellulose derivatives (HPMCAS, CMCAB and CAAdP). The dispersions were characterized by FT-IR, DSC, XRPD and ^{1}H NMR. Solubility and stability enhancement were studied using UV–vis spectrometry. Results were compared with those of crystalline Que, physical polymer/Que mixtures, and Que/PVP solid dispersions.

2. Experimental

2.1. Chemicals

Quercetin (hydrate, ≥95%) was purchased from Aldrich Chemicals. PVP (K29-32, MW 58,000) and KBr (99+%, for spectroscopy, IR grade) were supplied by Acros Organics (Geel, Belgium). CMCAB (641-0.2) was from Eastman Chemical Company. HPMCAS (AS-LG) was from Shin-Etsu Chemical Co., Ltd. (Tokyo, Japan). CAAdP (DS(acetyl) = 0.04, DS(propionyl) = 2.09, DS(adipate) = 0.33) was synthesized from commercial cellulose acetate propionate as we have previously described (Kar, Liu, & Edgar, 2011). Acetone (HPLC grade, 0.2 micron filtered), reagent alcohol (ethanol), potassium phosphate monobasic, and sodium hydroxide were supplied by Fisher Scientific (Fair Lawn, NJ). Buffers (pH 6.8, 1.2) were prepared according to USP30-NF25.

2.2. Preparation of spray-dried solid dispersions

Que/polymer mixtures (10.0 g) in different weight ratios (1:9, 1:3, 1:1, 3:1 and 9:1) were dissolved in acetone/ethanol (1/4, 500 mL) to make 2 wt% solutions. ASDs were prepared using a Buchi mini-spray dryer B-290. Operating parameters were: inlet temperature, 90 °C; outlet temperature, 57–60 °C; feed rate, 9 mL/min; nitrogen flow 350 L/h. Spray-drying process weight yields were approximately 50–60%.

Physical mixtures of Que and polymers were made by grinding weighed mixtures together with a mortar and pestle.

2.3. Characterization of the spray-dried quercetin/matrix solid dispersions

Que/polymer ASDs were characterized by comparing FTIR spectra, NMR spectra, DSC traces, and XRPD patterns to those from crystalline Que, polymers, and physical mixtures of Que/polymer.

2.3.1. IR spectroscopy

IR spectra were recorded between 4000 and 400 cm^{-1}, using a resolution of 4 cm^{-1} and 40 accumulations, on a Nicolet 8700 FT-IR Spectrometer. Pellets were prepared from sample/KBr mixtures (1:100 weight ratio).

2.3.2. NMR spectroscopy

^{1}H NMR spectra were recorded on an Inova 400 M instrument in acetone-d_6 with TMS as internal reference. Solid-state CP MAS ^{13}C NMR experiments were performed at 75.47 MHz on a BRUKER Avance II 300 spectrometer equipped with a MAS probe head using 4 mm ZrO_2 rotors. Glycine was used to set the Hartmann–Hahn conditions and adamantane as secondary chemical shift reference δ = 38.48 ppm and 29.46 ppm from external TMS respectively. Conventional spectra were recorded with a proton 90° pulse length of 4.0 μs and a contact time of 1 ms. Repetition delay was 10 s,

spin rate was 7 kHz, scan number 512 within 1.5 h, and spectral width 25 kHz. FIDs were accumulated with time domain size of 1k data points. RAMP shape pulse was used during cross-polarization and spinal64 for decoupling during acquisition. Spectral data were processed using Topspin program.

2.3.3. XRPD analysis

XRPD measurements used a Bruker D8 Discovery X-ray diffractometer. Measurements were performed at 40 kV voltage and 25 mA. Scanned angle was set as $5 < 2\theta < 40^\circ$ and scan rate was 2°/min.

2.3.4. DSC measurement

Heating curves of Que and solid dispersions were obtained using a modulated differential scanning calorimeter (Model Q2000, TA Instruments, New Castle, Delaware) equipped with refrigerated cooling accessory. Sample (2–5 mg) was packed in a non-hermetically crimped aluminum pan, and heated under dry nitrogen purge. Samples were heated from 25 °C to 100–120 °C at 10 °C/min to eliminate moisture and relieve stress, quickly cooled to 25 °C at 100 °C/min, then heated from 25 °C to 200 °C at 10 °C/min; transitions are reported from the second heating scan. DSC heating curves were analyzed using Universal Analysis 2000 software (TA Instruments).

2.4. UV–vis spectroscopy

All UV–vis spectra were recorded on a Thermo Scientific Evolution 300 UV–visible spectrometer.

2.5. Measurement of matrix polymer solubility

Polymer (0.5 g; CMCAB, HPMCAS, CAAdP or PVP) was dispersed in 10 mL of pH 6.8 buffer. The suspension was vortex-mixed for 1 min, ultrasonicated for 15 min, then shaken for 24 h at room temperature (Burrell wrist action shaker Model 75). The suspension/solution was centrifuged at 14,000 × *g* for 10 min to remove insoluble material. An aliquot (1 mL) of the top, clear solution was withdrawn and solvent was evaporated in an oven (80 °C, 5 h). Dissolved polymer weight was calculated by subtracting the weight of salt in buffer solution (7.7 mg/mL calculated from the weight of potassium phosphate monobasic and NaOH in 1 L pH 6.8 buffer) from the residue weight. Dissolved polymer concentration (w/v) was calculated by dividing dissolved polymer weight by the volume of solution withdrawn.

2.6. Que calibration curves in ethanol and pH 6.8 buffer

It is a challenge to create a calibration curve for a poorly soluble drug like Que that covers supersaturated concentrations expected from ASDs. From Que standard curves (Supplementary Material S1), its extinction coefficient changes only slightly in going from ethanol (55 L g^{-1} cm^{-1}) to pH 6.8 buffer (50 L g^{-1} cm^{-1}). Que extinction coefficients in pH 6.8 buffer are similar in the presence of dissolved (0.63 μg/mL) matrix polymers (HPMCAS 52, PVP 49). We employed ethanol UV–vis calibration curves to avoid issues arising from crystallization and nanoparticles.

A standard curve in ethanol was generated for calculation of Que concentration by UV–vis absorption. Calibration curves in aqueous buffer (pH 6.8) were generated by dilution of Que solution in ethanol (1.0 mg/mL, 10–200 μl) with pH 6.8 buffer to 10 mL. To study the effect of polymer matrix on the standard curve, Que/ethanol stock solution (1 mg/mL) was diluted by the solution of HPMCAS or PVP (0.63 mg/mL) in pH 6.8 buffer.

2.7. Dissolution testing – maximum Que solution concentration

Solid dispersion (Que content fixed at 50 mg) was dispersed in 10 mL of pH 6.8 phosphate buffer in an amber flask with shaking until equilibrium was reached (as determined by a measured plateau in [Que]). Then the suspension was centrifuged at 14,000 × *g* for 10 min to remove any insoluble material. Que supernatant concentration was determined by UV–vis spectrometry using the calibration curve in ethanol generated as described above.

2.8. Measurement of Que stability

Que stability enhancement by polymers in solution was studied by UV–vis spectrometry. Que and Que/PVP (1/9) solid dispersion were dissolved in ethanol, while Que/HPMCAS, Que/CMCAB and Que/CAAdP (1/9) solid dispersions was dissolved in tetrahydrofuran (THF) due to the low solubility of cellulose derivatives in ethanol, with Que concentration fixed at 1 mg/mL. Each stock solution (200 μL) was diluted to 10 mL with pH 6.8 buffer solution. UV–vis absorption of diluted solutions was measured at time intervals from 0.5 to 24 h.

The following experiments were designed to study Que recrystallization in aqueous buffer. Aliquots (40 μL) of 1 mg/mL Que or Que/polymer 1/9 solid dispersion ([Que] = 1 mg/mL; dissolved in ethanol or THF) were added to pH 6.8 buffer (960 μL, 0.2 M). Samples were incubated at room temperature for the indicated times. After incubation, the mixtures were diluted (1 mL EtOH) and UV–vis absorption of the diluted clear solution was measured.

The following experiments addressed Que degradation in aqueous buffer. Aliquots (4 mL, 1 mg/mL Que or Que/polymer 1/9 solid dispersions ([Que] = 1 mg/mL; dissolved in ethanol or THF) were added to pH 6.8 buffer (96 mL, 0.2 M). Samples were incubated at room temperature for 24 h. After incubation, the mixture was extracted with ethyl acetate (100 mL × 2). Combined organic layers were dried over sodium sulfate, then condensed by rotary evaporation. The residue was dissolved in ethanol and dialyzed against ethanol to remove polymer; the dialysate contained the Que and degradation products. The ethanol dialysate was condensed to dryness and the residue was analyzed by GC–MS.

2.9. GC–MS analysis

To 50–100 μg of extracted sample was added 50–100 μL of N,O-bis(trimethylsilyl) trifluoroacetamide (BSTFA) as silylation reagent. The mixture was heated at 70 °C for 20 min. Gas chromatography was performed on a HP 5890 instrument equipped with a Restek Rtx-5MS 30 m × 0.32 mm × 0.25 um column. Injector temperature was 250 °C. Helium carrier gas pressure was 7 psi. The temperature program used was as follows: 80–280 °C at 8 °C/min. Mass spectra were acquired on a VG 70 SE instrument. Electron ionization was achieved at 70 eV, and the source temperature was 150–200 °C. The mass range was scanned from *m*/*z* 75 to 750 in 1.5 s.

2.10. Que dissolution – release profile

Que/polymer samples (physical mixture or ASD) were dispersed in pH 6.8 buffer (100 mL) in amber glass flasks with fixed 0.07 mg/mL Que concentration, and stirred with a stir bar at 25 °C. Aliquots (1.5 mL) were withdrawn at appropriate time intervals and replaced with 1.5 mL of fresh dissolution medium to maintain constant volume. Aliquot UV–vis absorption was recorded after centrifugation at 4550 × *g*, 14,000 × *g* or 70,000 × *g* for 10 min. Drug release profiles in pH 1.2 buffer of Que, and 1/9 ASDs of Que

in polymers were measured using the same method, and aliquots were centrifuged at 14,000 × *g* before UV–vis measurement.

3. Results and discussion

We selected three promising carboxylated cellulose derivatives as the polymer matrices for preparation of Que solid dispersions. CMCAB is a relatively hydrophobic carboxylated cellulose ester that has shown promise for ASD solubility enhancement of hydrophobic drugs like griseofulvin and glyburide (Posey-Dowty et al., 2007; Shelton et al., 2009). HPMCAS has been the subject of a great deal of recent interest as an ASD polymer (Friesen et al., 2008), is somewhat more hydrophilic and water-soluble than CMCAB, and is included in multiple new drug application filings. CAAdP is the product of structure–property studies carried out by the Edgar and Taylor laboratories, for the purpose of designing effective ASD polymers, and has shown excellent ability to inhibit crystal growth of the poorly soluble drug ritonavir (Ilevbare et al., 2012). These carboxylated polymers may not only stabilize amorphous Que in solid and solution states, but also provide triggered release at small intestine pH. The hydrophobicity and solubility of these modified polysaccharides may affect their ability to stabilize and solubilize Que. The results were compared with those from ASDs employing the water-soluble polymer PVP; PVP has long been known as an effective polymer for drug solubility enhancement using the ASD method, particularly for cases where pH-sensitive release is not required (Simonelli, Mehta, & Higuchi, 1969).

3.1. Characterization of amorphous solid dispersions

We evaluated the relative abilities of these polymers to stabilize against crystallization in the solid phase by preparing spray-dried Que dispersions of various concentrations and comparing with physical blends of equal composition.

XRPD was used to investigate the crystallinity of Que/polymer matrices. XRPD patterns of all Que/CMCAB physical mixtures (Fig. 2) are similar to that of crystalline Que, with intensity proportional to %Que; this indicated the continuing presence and the ability to detect crystalline Que at as little as 10 wt%. In contrast, quercetin/CMCAB spray dried blends (up to 50 wt% Que) showed a halo pattern without any diffraction peaks, indicating that Que is completely amorphous. However, XRPD patterns of higher concentration (75 and 90 wt% Que) ASDs show weak diffraction peaks, indicating partial Que crystallinity. HPMCAS spray dried dispersions were X-ray amorphous up to 50 wt% Que, but crystalline peaks were observed in all physical mixtures; we also subjected 1/9 dispersions of Que in PVP and CAAdP to XRPD analysis, which again showed no evidence of crystallinity.

DSC provides information not only about the physical state of the drug in the blend, but also the polymer physical state. In the case of polysaccharides containing both pendent carboxyl and hydroxyl groups (e.g. CMCAB, HPMCAS, CAAdP) DSC transitions are observed above 200 °C that we ascribe to crosslinking esterification reactions. Therefore it is important to carry out DSC analyses of mixtures containing these polymers at temperatures not greater than about 200 °C. DSC second heating curves of quercetin/CMCAB dispersions ([Que] up to 50 wt%) as well as those of pure components are shown in Fig. 3(A), and the T_g values of dispersions are plotted versus Que content (Fig. 3(B)). Que used in these studies melted at 326 °C. Polymer matrix T_g values were 141 °C (CMCAB), 133 °C (CAAdP), 121 °C (HPMCAS) and 175 °C (PVP). T_g values of Que spray-dried dispersions decreased compared those of pure polymer matrices and decreased with increasing [Que] (Fig. 3), typical for a small molecule plasticizer molecularly dispersed in a polymer matrix. An exothermic peak at around 180 °C was observed for Que/HPMCAS (1/1) and Que/CMCAB (1/3) SDs, indicating high-temperature Que crystallization during the DSC experiment.

FTIR was used to explore quercetin–polymer interactions in the matrix. IR spectra of quercetin, HPMCAS, Cur/HPMCAS (1:1) physical mixtures and spray dried solid dispersions are shown in Fig. 4(A). The band at 3300–3500 cm^{-1} was attributed to Que–OH stretching. In the physical mixture this band shape does not change and the sharp peaks at 3323 and 3405 cm^{-1} can be observed clearly. However, the spray dried dispersion shows broad peaks at 3300–3500 cm^{-1}, similar to the bands of pure HPMCAS. This significant peak broadening may be attributed to the intermolecular hydrogen bonding (H-bonding) between Que and the matrix polymer, which may aid disruption of Que crystalline structure. Pure HPMCAS shows a strong absorption at 1747 cm^{-1} (C=O stretch). In spray-dried HPMCAS/Que this peak shifted slightly to 1734 cm^{-1}, also indicative of H-bonding interaction between Que and HPMCAS. FTIR spectra of Que/HPMCAS ASDs vs. Que concentration are shown in Fig. 4(B). Sharp peaks at 3323 and 3405 cm^{-1} appeared in the spectra of ASDs with Que concentration > 50 wt%, indicating that Que is only partly amorphous in these solid dispersions, in agreement with the XRPD analysis.

Solid-state CPMAS ^{13}C NMR was also used to study Que/matrix interaction. CPMAS ^{13}C NMR spectra of CMCAB, Que and Que/CMCAB 1/3 ASD are shown in Supplementary Materials S2(B). The Que spectrum was assigned in accordance with the literature (Olejniczak & Potrzebowski, 2004; Wawer & Zielinska, 1997). Carbons with single bonds to oxygen appear between 110 and 165 ppm. H-bonding between Que and polymer may change the peak shapes and/or shifts of such carbons. Since this region is vacant in the CMCAB spectrum, changes due to Que/polymer interactions are clearly distinguishable. In the solid dispersion spectra all the peak shapes became broadened (e.g. C3 (136 ppm), C9 (157 ppm)). Some peaks merged to form broad peaks (e.g., C2′ and C5′; C1′ and C6′; C2, 4′ and 3′; C5 and C7). Some chemical shift changes are evident (e.g., C7 (Que 164 ppm, Que/CMCAB 1/3 SD 163 ppm) and C3′ (Que 142 ppm, Que/CMCAB 1/3 SD 145 ppm). C5 experiences the largest chemical shift change, from 155 ppm (Que) to 161 ppm (Que/CMCAB 1/3 SD). It should be noted that all carbons with obvious chemical shift changes bear hydroxyl groups, which may form H-bonds with the matrix polymer. Similar changes were observed between Que and its solid dispersions in the other polymers by ^{13}C CPMAS (data not shown). The observed changes in peak shape and chemical shift support substantial Que–polymer H-bonding in these ASDs.

^{1}H NMR spectra of ASDs were examined to confirm the lack of chemical reaction between Que and polymer (see Supplementary Material S2(A)). Spectra are simply additive of those of the pure components, with no new peaks or significant resonance shifts. They support the conclusion that Que is chemically unreactive with these matrix polymers under our spray-drying conditions.

3.2. Study of quercetin degradation

It has been reported that Que is rapidly degraded in aqueous solution at pH ≥ 5 (Zheng et al., 2005). Zenkevich et al. studied Que aerobic degradation at pH 10 (Zenkevich et al., 2007). They found that 3,4-dihydroxybenzoic acid (A), 2,4,6-trihydroxybenzoic acid (B) and phloroglucinol are the main degradation products and proposed a mechanism involving dioxygen addition (S3). Recently, investigators have reported protection of Que from alkaline degradation by formulation as lecithin-based nanoparticles (Date et al., 2011). Dissolution of molecularly dispersed curcumin, a related flavonoid, in HPMCAS has been observed to accelerate photochemical degradation in comparison with that of crystalline curcumin, and stabilize it only slightly in comparison with dissolved pure curcumin (Onoue et al., 2010). To study degradation and the inhibitory

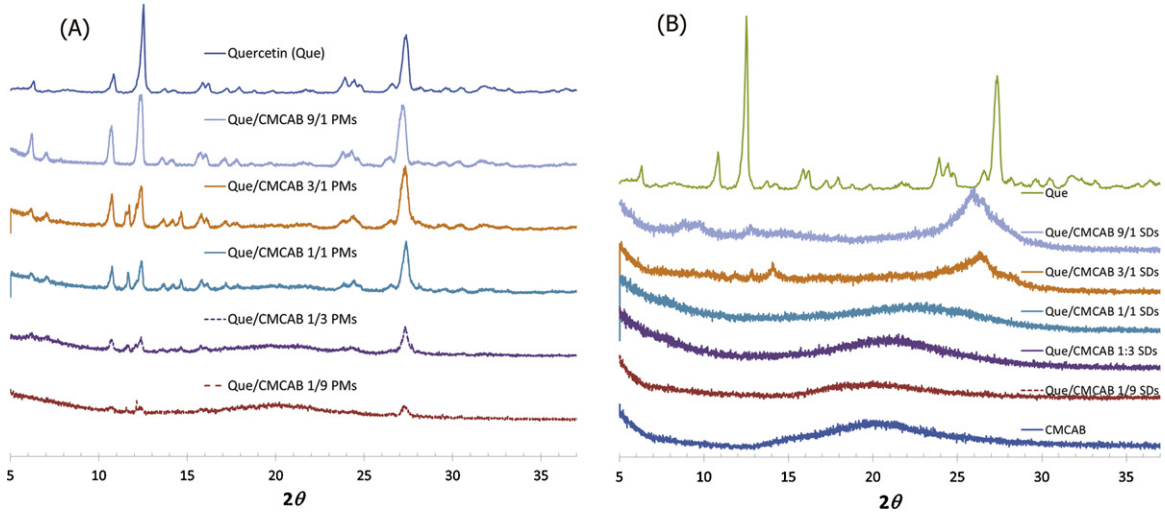

Fig. 2. XRPD spectra of Que/CMCAB physical mixtures (A) and solid dispersions (B).

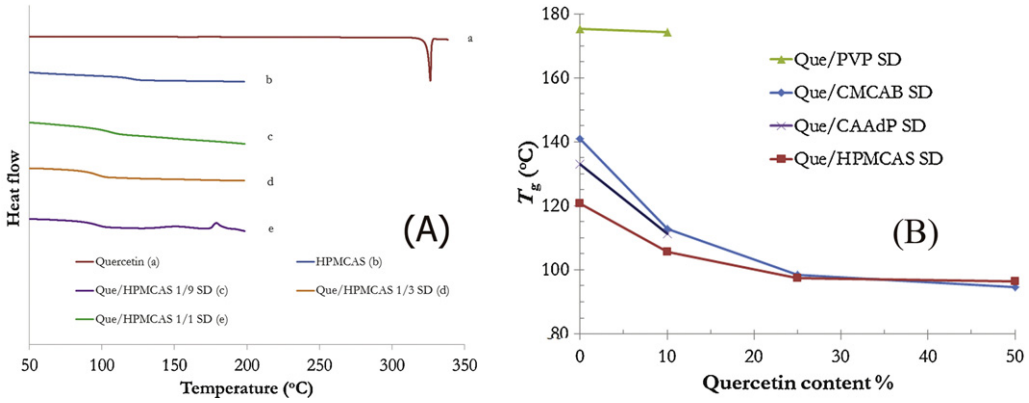

Fig. 3. (A) DSC second heating curves of Que, HPMCAS, 1:1 Que physical mixture and solid dispersion; (B) T_g values Que solid dispersions vs. Que content.

effect of polymer matrices, Que and its ASDs (Que/polymer 1/9) were incubated in pH 6.8 buffer (24 h, room temperature). After extraction with ethyl acetate and dialysis in ethanol to remove polymer, the residue was characterized by GC-MS (Supporting Materials S4, S5). As can be seen from S4 and S5, little degradation was observed for pure Que and Que/PVP 1/9 SD, while degradation products (A and B) were found for ASDs in the cellulose ester matrices. Furthermore Que degradation in CAAdP ASD appears to be rapid since nearly no Que was detected by GC/MS after pH 6.8 incubation. These results are in stark contrast to those observed in our labs with similar ASDs of curcumin, where these same cellulose ester polymers strongly stabilized curcumin against alkaline degradation (Li, Konecke, Wegiel, Taylor, & Edgar, under review). A possible explanation for the very different influences of polymers on Que vs. curcumin degradation may be that curcumin degradation is via retro-aldol mechanism, involving an ionic transition state

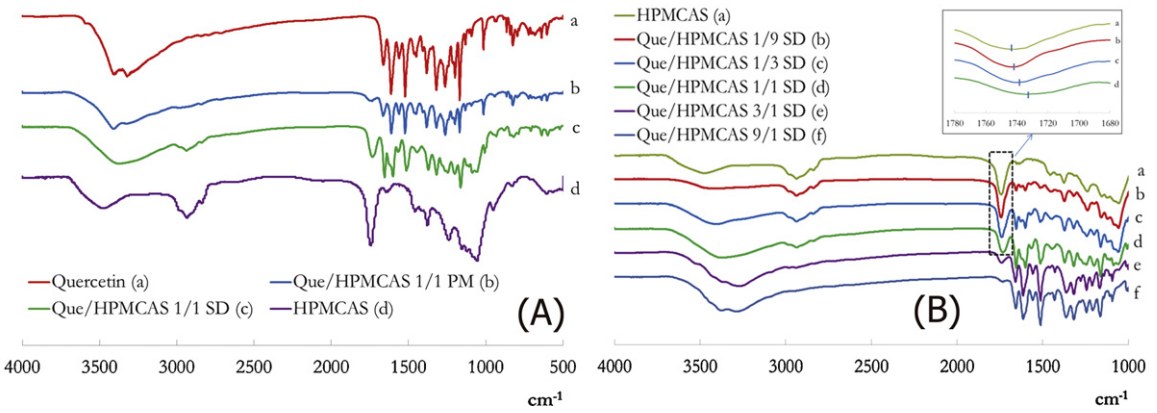

Fig. 4. (A) FTIR spectra of Que, HPMCAS, 1:1 Que/HPMCAS physical mixture and solid dispersion; (B) FTIR spectra of HPMCAS and Que/HPMCAS solid dispersions of varying composition.

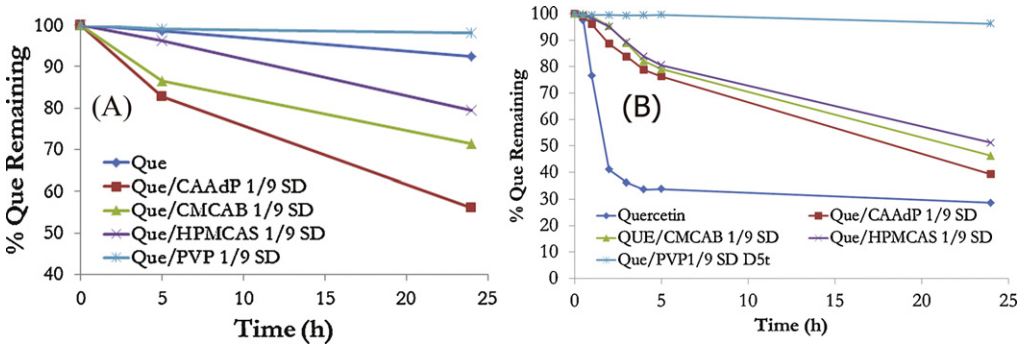

Fig. 5. (A) Stability of Que and Que/polymer solid dispersions at pH 6.8 by UV-Vis (EtOH added); (B) Stability of Que and Que/polymer solid dispersions at pH 6.8 by UV-Vis (no EtOH added).

Table 1
Degradation and precipitation of Que vs. ASD polymer.

Polymer	Que degradation (%)	Que crystallization (%)
None	8	64
PVP	2	2
HPMCAS	21	28
CMCAB	29	26
CAAdP	44	17

that may be retarded in the hydrophobic cellulose ester matrix. In contrast, the Que degradation, involving reaction with non-polar oxygen, could be enhanced in a hydrophobic matrix.

Polymer impact on degradation was further confirmed by UV–vis analysis of Que in buffer (pH 6.8); samples were diluted with ethanol just prior to measurement. After 24 h (Fig. 5(A)), concentration of pure Que dropped 8%, and in Que/PVP ASD (1/9), [Que] dropped only 2%. The relative stability of pure Que could be due to fast crystallization from aqueous buffer, protecting it from degradation. Loss of Que from cellulosic ASDs was more rapid (HPMCAS 21%, CMCAB 29%, CAAdP 44%). The degradation rate in polymer ASD seems to correlate with polymer hydrophobicity (and aqueous solubility), and would be consistent with a mechanism in which O_2 permeation into the matrix was a key step. Certainly more experiments are needed before we can fully understand the mechanism by which polymers impact Que degradation upon release from ASDs.

The contribution of precipitation to Que removal from solution is illustrated in Fig. 5(B), which shows UV–vis absorption of ASDs in pH 6.8 buffer (without ethanol dilution) versus time. Solution concentration of pure Que decreased rapidly, with only around 34% remaining after 5 h. As we have seen (Fig. 5(A)), Que chemical degradation under these conditions is much slower (8% after 5 h), indicating that precipitation is the dominant effect. While 71% of pure Que had degraded or crystallized within 24 h, Que in PVP ASD was far more stable (only 4% lost from solution). The cellulose derivative-based ASDs did not stabilize Que in solution as effectively; only 51% (HPMCAS), 46% (CMCAB), or 39% (CAAdP) Que remaining in solution after 24 h at pH 6.8. Taking the results of these two sets of experiments together, we can estimate the impacts of chemical degradation and crystallization on the loss of dissolved Que after 24 h (Table 1). Separation of degradation and precipitation effects is important to help us design effective ASD systems.

3.3. Dissolution testing and solution concentration enhancement

Dissolution of Que from ASDs can afford complex mixtures, including micro- and nano-particles and aggregates along with the dissolved drug, polymer and drug–polymer complex. The fact that nanoparticles absorb UV light can lead to over-estimation of

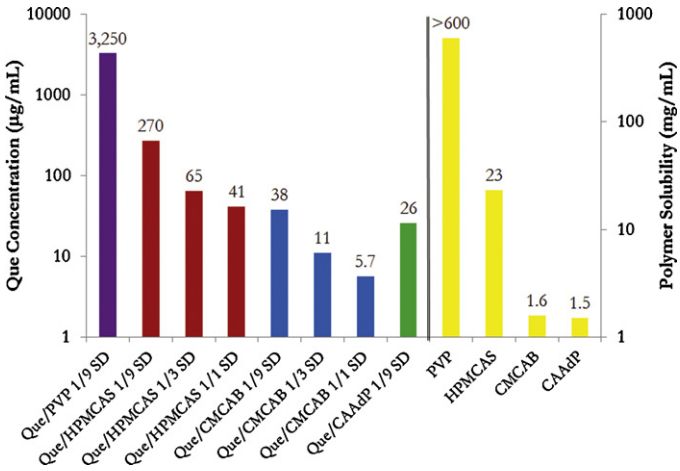

Fig. 6. Maximum Que solution concentration vs. dispersion (L axis) and polymer solubility (R axis) at pH 6.8.

the dissolved active concentration (Bohren & Huffman, 1983). We would like to reliably remove such particles to permit accurate UV quantification of dissolved drug. Filtration is a common approach, but it is not a reliable method as commercial filters may not remove nanoparticles of <20 nm diameter, and non-polar drugs may be adsorbed onto the filter material (Lindenberg, Wiegand, & Dressman, 2005). As mentioned previously, calibration curves of poorly soluble drugs like Que at supersaturated concentrations in the absence of polymer are also a hurdle, but we dealt with this issue in the dissolution experiments by using the ethanol calibration curve protocol previously discussed.

We turned to centrifugation in order to remove nanoparticles from samples prior to dissolved [Que] measurements. We knew from our previous studies with curcumin (Li et al., under review) that centrifugation at 14,000 × *g* was adequate to give consistently good results, and was experimentally convenient for us (see Supporting Information S6, S7). This protocol gave repeatable values for [Que] with standard deviation 3–5% in triplicate experiments. In the dissolution tests, Que ASD was dispersed in pH 6.8 buffer solution with a fixed maximum Que concentration of 5 mg/mL. After equilibrium was reached, Que concentration was measured by UV–vis analysis of the supernatant from centrifugation (Fig. 6). Clearly molecular dispersions with lower Que concentration afford higher Que solution concentrations, as is typical of amorphous dispersion formulations (Simonelli et al., 1969; Simonelli, Mehta, & Higuchi, 1976). Solution concentrations from HPMCAS dispersions are uniformly much higher than from equivalent CMCAB dispersions. The higher aqueous solubility of HPMCAS than either CMCAB or CAAdP is very likely an important influence on the maximum Que

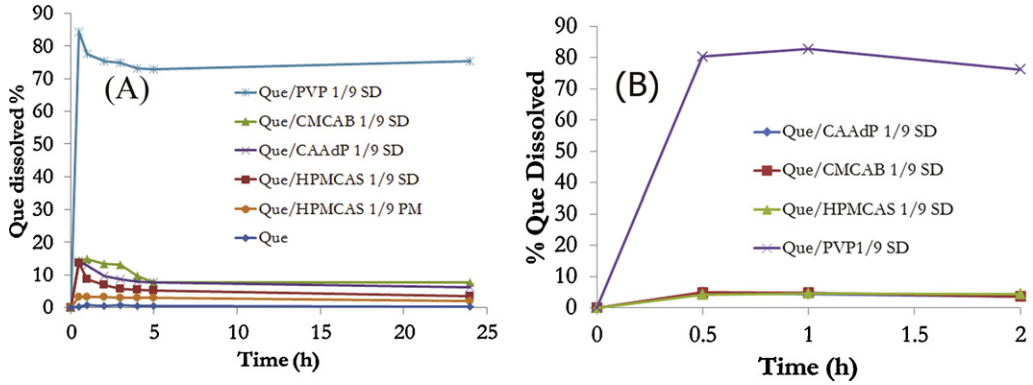

Fig. 7.

concentration attained from these ASDs (Fig. 6). The solubility of cellulose derivatives impacts Que solution concentration because Que release is a result of pH-triggered swelling and/or dissolution of the polymer. In addition, high concentrations of dissolved polymer may change Que solubility by thermodynamic effects.

3.4. Drug release profiles

In the measurement of drug release profiles, maximum Que concentration was fixed at 0.07 mg/mL in pH 6.8 buffer solution. The UV–vis absorption of the solution was measured and plotted vs. time.

Drug release profiles of Que/HPMCAS and Que/CMCAB ASDs in pH 6.8 buffer are shown in Fig. S8 (A and B). Fastest and most extensive release was observed at the lowest Que concentrations in the CMCAB ASDs. At 1:9 quercetin/CMCAB the highest release (15%) was observed within 1 h, vs. only 5% release from a 1:1 dispersion. Recent reports indicate that Que/PVP solid dispersions follow the same tendency (Zhu et al., 2007). However, all three Que/HPMCAS ASDs gave similar Que release profiles. Within 0.5 h, Que released reached 13–14%, then decreased rapidly to 4–5% within 5 h.

In order to understand the influence of polymer matrix upon release, drug release profiles at pH 6.8 from Que/PVP 1/9, Que/HPMCAS 1/9, Que/CMCAB 1/9 and Que/CAAdP 1/9 solid dispersions were compared (Fig. 7(A)) with dissolution of pure quercetin and from a physical mixture (Que/HPMCAS 1/9). Release from the Que/PVP 1/9 solid dispersion was fastest and most complete, reaching 84% within 0.5 h, while release from the Que/HPMCAS, CMCAB or CAAdP blends (1/9 SD) was quite slow and incomplete, reaching a maximum of only 14% after 0.5 h. In contrast, dissolution of pure Que and release from Que/HPMCAS 1/9 physical mixture were much slower and less complete than that from the ASDs, reaching only 0.7% and 3% respectively after 1 h. Clearly PVP is highly effective at suppressing quercetin crystallization in both the solid and solution phases, and effectively releases Que at pH 6.8, leading to practical Que levels within physiologically relevant time windows. In contrast, all three cellulose derivative matrices display similarly slow drug release, while still much faster and more complete than pure Que and the Que/polymer physical mixture.

It is also of interest to compare Que release from these solid dispersions under conditions similar to those of the stomach, in pH 1.2 buffer (Fig. 7(B)). Release from the PVP amorphous blend (Que/PVP 1/9 SD blend) was substantial, reaching 80% Que release within 1 h. In contrast, only 5% Que release was observed from quercetin amorphous blends with CMCAB, CAAdP, or HPMCAS. Since PVP contains a slightly basic amide group in contrast to the pendent carboxyls of the cellulose esters, this result is exactly what we would expect chemically. We can expect that CMCAB, CAAdP and HPMCAS would isolate Que from the stomach contents much more effectively than would PVP.

4. Conclusions

Quercetin and the cellulose esters CMCAB, CAAdP and HPMCAS were readily blended by spray-drying, affording amorphous solid dispersions with Que content up to 50%. Release from HPMCAS, CMCAB and CAAdP dispersions was quite slow and incomplete, probably due to the low wettability and poor water solubility of these polysaccharide derivatives. In contrast, release from PVP matrices was much faster and more complete. Cellulose derivative matrices did provide pH-triggered release, in contrast with PVP matrices from which Que was released even at gastric pH. HPMCAS, CAAdP, CMCAB and PVP all inhibited Que crystallization from solution, but only PVP prevented Que chemical degradation, perhaps due to the higher hydrophilicity of PVP vs. the cellulose derivatives. Indeed, the three cellulose derivatives appeared to accelerate Que degradation, in contrast to the stabilization by PVP. This is surprising since we have found that cellulose esters such as CAAdP provide effective stabilization of curcumin against the chemical degradation to which it is quite prone (manuscript from our labs under review). Systems based on these solid dispersions are promising for development of enhanced-bioavailability, quercetin-based therapeutic and dietary supplement formulations. It will be of interest to see whether these *in vitro* results will translate into improved *in vivo* bioavailability, permitting detailed analysis of the pharmacokinetics and pharmacodynamics of this fascinating bioactive flavonoid.

Acknowledgements

We thank USDA (grant number 09-35603-05068) for financial support and the Virginia Tech Institute for Critical Technologies and Applied Science (ICTAS) for their support of this project. We thank Eastman Chemical Company and Shin-Etsu Ltd. for their gracious donations of CMCAB and HPMCAS, respectively.

Appendix A. Supplementary data

Supplementary data associated with this article can be found, in the online version, at http://dx.doi.org/10.1016/j.carbpol.2012.11.073.

References

Andersen, Ø. M., & Markham, K. R. (2006). *Flavonoids: chemistry, biochemistry, and applications*. Boca Raton, FL: CRC, Taylor & Francis.

Biasutto, L., Marotta, E., De Marchi, U., Zoratti, M., & Paradisi, C. (2006). Ester-based precursors to increase the bioavailability of quercetin. *Journal of Medicinal Chemistry*, *50*, 241–253.

Biasutto, L., Marotta, E., Garbisa, S., Zoratti, M., & Paradisi, C. (2010). Determination of quercetin and resveratrol in whole blood-implications for bioavailability studies. *Molecules*, *15*, 6570–6579.

Bischoff, S. C. (2008). Quercetin: Potentials in the prevention and therapy of disease. *Current Opinion in Clinical Nutrition and Metabolic Care*, *11*, 733–740.

Bohren, C. F., & Huffman, D. R. (1983). *Absorption and scattering of light by small particles*. New York: John Wiley and Sons.

Chen, C., Zhou, J., & Ji, C. (2010). Quercetin: A potential drug to reverse multidrug resistance. *Life Sciences*, *87*, 333–338.

Chien, S.-Y., Wu, Y.-C., Chung, J.-G., Yang, J.-S., Lu, H.-F., Tsou, M.-F., et al. (2009). Quercetin-induced apoptosis acts through mitochondrial- and caspase-3-dependent pathways in human breast cancer MDA-MB-231 cells. *Human & Experimental Toxicology*, *28*, 493–503.

Costa, A. R. d. M., Marquiafavel, F. S., Vaz, M. M. d. O. L. L., Rocha, B. A., Bueno, P. C. P., Amaral, P. L. M., et al. (2011). Quercetin-PVP K25 solid dispersions. *Journal of Thermal Analysis and Calorimetry*, *104*, 273–278.

Date, A. A., Nagarsenker, M. S., Patere, S., Dhawan, V., Gude, R. P., Hassan, P. A., et al. (2011). Lecithin-based novel cationic nanocarriers (Leciplex) II: Improving therapeutic efficacy of quercetin on oral administration. *Molecular Pharmaceutics*, *8*, 716–726.

DiNunzio, J. C., Miller, D. A., Yang, W., McGinity, J. W., & Williams, R. O. (2008). Amorphous compositions using concentration enhancing polymers for improved bioavailability of itraconazole. *Molecular Pharmaceutics*, *5*, 968–980.

Friesen, D. T., Shanker, R., Crew, M., Smithey, D. T., Curatolo, W. J., & Nightingale, J. A. (2008). Hydroxypropyl methylcellulose acetate succinate-based spray-dried dispersions: An overview. *Molecular Pharmaceutics*, *5*, 1003–1019.

Gibellini, L., Pinti, M., Nasi, M., De, B. S., Roat, E., Bertoncelli, L., et al. (2010). Interfering with ROS metabolism in cancer cells: The potential role of quercetin. *Cancers*, *2*, 1288–1311.

Ilevbare, G. A., Liu, H., Edgar, K. J., & Taylor, L. S. (2012). Understanding polymer properties important for crystal growth inhibition—impact of chemically diverse polymers on solution crystal growth of ritonavir. *Crystal Growth & Design*, *12*, 3133–3143.

Jan, A. T., Kamli, M. R., Murtaza, I., Singh, J. B., Ali, A., & Haq, Q. M. R. (2010). Dietary flavonoid quercetin and associated health benefits—an overview. *Food Reviews International*, *26*, 302–317.

Kar, N., Liu, H., & Edgar, K. J. (2011). Synthesis of cellulose adipate derivatives. *Biomacromolecules*, *12*, 1106–1115.

Kelly, G. S. (2011). Quercetin. *Alternative Medicine Review*, *16*, 172–194.

Kuo, S.-M. (2002). Flavonoids and gene expression in mammalian cells. *Advances in Experimental Medicine and Biology*, *505*, 191–200.

Lamson, D. W., & Brignall, M. S. (2000). Antioxidants and cancer III. Quercetin. *Alternative Medicine Review*, *5*, 196–208.

Lauro, M. R., Maggi, L., Conte, U., De, S. F., & Aquino, R. P. (2005). Rutin and quercetin gastro-resistant microparticles obtained by spray-drying technique. *Journal of Drug Delivery Science and Technology*, *15*, 363–369.

Lauro, M. R., Torre, M. L., Maggi, L., De, S. F., Conte, U., & Aquino, R. P. (2002). Fast- and slow-release tablets for oral administration of flavonoids: Rutin and quercetin. *Drug Development and Industrial Pharmacy*, *28*, 371–379.

Leuner, C., & Dressman, J. (2000). Improving drug solubility for oral delivery using solid dispersions. *European Journal of Pharmaceutics and Biopharmaceutics*, *50*, 47–60.

Li, B., Konecke, S., Wegiel, L., Taylor, L. S., & Edgar, K. J. (under review). Both solubility and chemical stability of curcumin are enhanced by solid dispersion in cellulose derivative matrices.

Li, B., Zhang, L., Deng, Y., & Liang, N. (2004). Study on solid dispersion of quercetin – PEG(6000). *Huaxi Yaoxue Zazhi*, *19*, 35–37.

Li, Y.-L., Yang, Y., Bai, T.-C., & Zhu, J.-J. (2010). Heat capacity for the binary system of quercetin and poly(vinylpyrrolidone) K30. *Journal of Chemical and Engineering Data*, *55*, 5856–5861.

Lindenberg, M., Wiegand, C., & Dressman, J. B. (2005). Comparison of the adsorption of several drugs to typical filter materials. *Dissolution Technologies*, *12*, 22–25.

Murakami, A., Ashida, H., & Terao, J. (2008). Multitargeted cancer prevention by quercetin. *Cancer Letters*, *269*, 315–325.

Olejniczak, S., & Potrzebowski, M. J. (2004). Solid state NMR studies and density functional theory (DFT) calculations of conformers of quercetin. *Organic & Biomolecular Chemistry*, *2*, 2315–2322.

Onoue, S., Takahashi, H., Kawabata, Y., Seto, Y., Hatanaka, J., Timmerman, B., et al. (2010). Formulation design and photochemical studies on nanocrystal solid dispersion of curcumin with improved oral bioavailability. *Journal of Pharmaceutical Sciences*, *99*, 1871–1881.

Posey-Dowty, J. D., Watterson, T. L., Wilson, A. K., Edgar, K. J., Shelton, M. C., & Lingerfelt, L. R. (2007). Zero-order release formulations using a novel cellulose ester. *Cellulose*, *14*, 73–83.

Qian, F., Huang, J., & Hussain, M. A. (2010). Drug–polymer solubility and miscibility: Stability consideration and practical challenges in amorphous solid dispersion development. *Journal of Pharmaceutical Sciences*, *99*, 2941–2947.

Ribeiro, M. E. N. P., Vieira, I. G. P., Cavalcante, I. M., Ricardo, N. M. P. S., Attwood, D., Yeates, S. G., et al. (2009). Solubilization of griseofulvin, quercetin and kurin in micellar formulations of triblock copolymers E62P39E62 and E137S18E137. *International Journal of Pharmaceutics*, *378*, 211–214.

Rice-Evans, C., & Packer, L. (2003). *Flavonoids in health and disease*. New York: Marcel Dekker.

Sansone, F., Picerno, P., Mencherini, T., Villecco, F., D'Ursi, A. M., Aquino, R. P., et al. (2010). Flavonoid microparticles by spray-drying: Influence of enhancers of the dissolution rate on properties and stability. *Journal of Food Engineering*, *103*, 188–196.

Shelton, M. C., Posey-Dowty, J. D., Lingerfelt, L. R., Kirk, S. K., Klein, S., & Edgar, K. J. (2009). Enhanced dissolution of poorly soluble drugs from solid dispersions in carboxymethylcellulose acetate butyrate matrices. In K. J. Edgar, T. Heinze, & T. Liebert (Eds.), *Polysaccharide materials: Performance by design* (pp. 93–113). Washington, D.C.: American Chemical Society.

Siegelin, M. D., Reuss, D. E., Habel, A., Rami, A., & von Deimling, A. (2009). Quercetin promotes degradation of survivin and thereby enhances death-receptor-mediated apoptosis in glioma cells. *Neuro-Oncology*, *11*, 122–131.

Simonelli, A. P., Mehta, S. C., & Higuchi, W. I. (1969). Dissolution rates of high energy polyvinylpyrrolidone (PVP)-sulfathiazole coprecipitates. *Journal of Pharmaceutical Sciences*, *58*, 538–549.

Simonelli, A. P., Mehta, S. C., & Higuchi, W. I. (1976). Dissolution rates of high energy sulfathiazole-povidone coprecipitates II: Characterization of form of drug controlling its dissolution rate via solubility studies. *Journal of Pharmaceutical Sciences*, *65*, 355–361.

Singh, M. C., Sayyad, A. B., & Sawant, S. D. (2010). Review on various techniques of solubility enhancement of poorly soluble drugs with special emphasis on solid dispersion. *Journal of Pharmacy Research*, *3*, 2494.

Timpe, C. (2010). Drug solubilization strategies: Applying nanoparticulate formulation and solid dispersion approaches in drug development. *American Pharmaceutical Review*, *13*, 12.

Tiwari, R. (2009). Solid dispersions: An overview to modify bioavailability of poorly water soluble drugs. *International journal of pharmtech research*, *1*, 1338.

Vargas, A. J., & Burd, R. (2010). Hormesis and synergy: Pathways and mechanisms of quercetin in cancer prevention and management. *Nutrition Reviews*, *68*, 418–428.

Wawer, I., & Zielinska, A. (1997). 13C-CP-MAS-NMR studies of flavonoids. I. Solid-state conformation of quercetin, quercetin 5′-sulphonic acid and some simple polyphenols. *Solid State Nuclear Magnetic Resonance*, *10*, 33–38.

Zenkevich, I. G., Eshchenko, A. Y., Makarova, S. V., Vitenberg, A. G., Dobryakov, Y. G., & Utsal, V. A. (2007). Identification of the products of oxidation of quercetin by air oxygen at ambient temperature. *Molecules*, *12*, 654–672.

Zheng, Y., & Chow, A. H. L. (2009). Production and characterization of a spray-dried hydroxypropyl-β-cyclodextrin/quercetin complex. *Drug Development and Industrial Pharmacy*, *35*, 727–734.

Zheng, Y., Haworth, I. S., Zuo, Z., Chow, M. S. S., & Chow, A. H. L. (2005). Physicochemical and structural characterization of quercetin-beta-cyclodextrin complexes. *Journal of Pharmaceutical Sciences*, *94*, 1079–1089.

Zhu, J., Yang, Z.-G., Chen, X.-M., Sun, J.-B., Awuti, G., Zhang, X., et al. (2007). Preparation and physicochemical characterization of solid dispersion of quercetin and polyvinylpyrrolidone. *Journal of Chinese Pharmaceutical Sciences*, *16*, 51–56.